Experimental and Molecular Pathology 107 (2019) 57–67

Contents lists available at ScienceDirect

Experimental and Molecular Pathology

journal homepage: www.elsevier.com/locate/yexmp

Knockdown on aPKC-ι inhibits epithelial-mesenchymal transition, migration and invasion of colorectal cancer cells through Rac1-JNK pathway

Guang-Sheng Du, Yuan Qiu, Wen-Sheng Wang, Ke Peng, Zhi-Cao Zhang, Xiang-Sheng Li, Wei-Dong Xiao*, Hua Yang*

Department of General Surgery, Xinqiao Hospital, Army Medical University, Chongqing 400037, PR China

ARTICLE INFO

Keywords:
Colorectal cancer
Atypical protein kinase C-ι
Epithelial-mesenchymal transition
Migration and invasion
Auranofin

ABSTRACT

Background: Atypical protein kinase C-ι (aPKC-ι) is an oncogenic factor, and required for the epithelial-mesenchymal transition (EMT) of different types of cancer. Our study aimed to investigate the role of aPKC-ι in the EMT, migration and invasion of colorectal cancer (CRC) cells.

Methods: Expression of aPKC-ι was evaluated in CRC cell lines treated with TGF-β1 using qPCR and western blot. After aPKC-ι was knocked down using shRNA, migration and invasion abilities of CRC cell lines were evaluated by wound healing assay and transwell assay, respectively. Activation status of downstream signaling factors of aPKC-ι, including Rac1, JNK, STAT3 and β-catenin, was measured using western blot. Furthermore, auranofin, an aPKC-ι inhibitor, was used to treat CRC cell lines to investigate its possible inhibition on the EMT of CRC cell lines, as well as on the expression of aPKC-ι and its downstream signaling factors.

Results: TGF-β1 induced the expression of aPKC-ι in CRC cells, and knockdown on aPKC-ι inhibited the TGF-β1-induced EMT, migration and invasion of CRC cells. Interestingly, Rac1 GTPase level was decreased when aPKC-ι was knocked down, and overexpression of Rac1G12V rescued the cell EMT, migration and invasion in CRC cells as inhibited by sh-aPKC-ι. Moreover, knockdown on aPKC-ι suppressed the phosphorylation of JNK and STAT3, and nuclear translocation of β-catenin. The aPKC- ι inhibitor, Auranofin, showed similar inhibitory effects as aPKC-ι knockdown.

Conclusion: Knockdown on aPKC-ι inhibited the EMT, migration and invasion of CRC cells through suppressing of Rac1-JNK pathway. Those findings indicate that aPKC-ι may serve as a novel therapeutic target for CRC.

1. Introduction

Development of distal metastatic lesions is the main cause of death in colorectal cancer (CRC) patients (Cho et al., 2012). Approximately 25% of the CRC patients show metastases when firstly diagnosed, with liver as the most affected organ, and half of the patients develop metastases during the whole disease course (Garden et al., 2006; Villalba et al., 2017). Compared to patients with localized CRC whose 5-year survival rate could approach 90%, those patients with metastatic CRC (mCRC) only have a 5-year survival rate of ~10% (Cho et al., 2012). In addition, if left untreated, mCRC patients only have a median overall survival of < 8 months (De Greef et al., 2016). Surgery is considered the standard of care for mCRC patients and offers the only potential for cure (Chiappa et al., 2009). However, only 10% ~ 20% of the mCRC patients are initially eligible for surgical treatment, and this number remains < 40% even after "conversion" therapies (De Greef et al., 2016). Due to the high metastasis rate in CRC patients and the high mortality rate behind it, it becomes quite necessary to study the underlying mechanism of CRC metastasis and find ways to control it.

Epithelial-mesenchymal transition (EMT) is known as the conversion of epithelial cells into cells with mesenchymal phenotype (Gurzu et al., 2016). Firstly known to be involved in embryogenesis and tissue repair, EMT was later found to play a role in the carcinogenesis and metastasis of tumors, including CRC (Thiery, 2003; Mjaatvedt and Markwald, 1989). Indeed, EMT was indicated as a pivotal mechanism of cancer cell invasion, through which tightly-bound epithelial cells acquire an invasive mesenchymal phenotype(Zhu et al., 2013). The hallmark changes of EMT in molecular level include the down-regulation of epithelial markers e.g. E-cadherin, claudins, α-catenin, γ-catenin, occludin, and the up-regulation of mesenchymal markers, e.g. N-cadherin, vimentin, Snail, the nuclear translocation of β-catenin, and etc., and the underlying pathways include transforming growth factor-β (TGF-β) pathway, Ras-mitogen-activated protein kinase/Snail/Slug pathway, NF-κB pathway, microRNAs, and etc. (Gurzu et al., 2016; Zhu

* Corresponding authors at: Department of General Surgery, Xinqiao Hospital, Army Medical University, Xinqiaozhengjie 183, Chongqing 400037, PR China.
E-mail addresses: Weidong.xiao@126.com (W.-D. Xiao), hwbyang@qq.com (H. Yang).

https://doi.org/10.1016/j.yexmp.2018.11.007
Received 31 July 2018; Received in revised form 7 November 2018; Accepted 17 November 2018
Available online 19 November 2018

et al., 2013; Gunaratne et al., 2013). Although many factors as mentioned above (e.g. E-cadherin) were used as immunohistochemistry markers for EMT, β-catenin remains the main oncoprotein of the EMT in CRC, and nuclear translocation of β-catenin serves as an important marker of EMT in CRC cells(Gurzu et al., 2016).Protein kinase C (PKC) family is a group of evolutionary-conserved serine/threonine kinases which was involved in different metabolic processes in almost all type of cells, and dysregulation of PKC could lead to different diseases, including diabetes, autoimmune diseases, cancer, and etc.(Isakov, 2018). PKC family could be divided into three subfamilies: conventional PKC (PKC-α, βI, βII and γ), novel PKC (PKC-δ, ε, η, θ), and atypical PKC (PKCζ and ι)(Bosco et al., 2011). Almost all of those PKC isoforms have been shown to exert cancer-promoting/inhibiting effects in different types of cancer, including breast cancer, colon cancer, lung cancer, pancreatic cancer, prostate cancer, gastrointestinal stromal tumor (GIST), glioma/glioblastoma, head and neck squamous cell carcinoma, hepatocellular carcinoma (HCC), leukemia, lymphoma, and etc.(Isakov, 2018). In addition, several PKC family members have been associated to EMT of tumor cells, e.g. PKC- θ in GIST(Kovecsi et al., 2017a; Kovecsi et al., 2017b), PKC- ε in breast cancer(Jain and Basu, 2014), and etc. In this study, we focused on PKC- ι, a member of atypical PKC, and its roles in EMT of CRC cells.

Atypical PKC-ι (aPKC-ι) has been reported to be functionally required for the EMT of different types of cancer, including lung, pancreatic, ovarian, prostate, colon and brain cancer(Murray et al., 2011). Previous studies reported that aPKC-ι-Par6 complex could activate Rac1 pathway which drives the transformed growth of non-small-cell lung cancer (NSCLC) (Gunaratne et al., 2013). In addition, aPKC-ι was also shown to enhance the phosphorylation of Par6 by TGF-β, therefore facilitating the EMT of the HCC (Ma et al., 2014; Du et al., 2009).

On the other hand, a group of anti-rheumatoid arthritis drugs could inhibit aPKC-ι by influencing its interaction with Par6, which was shown to inhibit the transformed growth of HCC and pancreatic cancer (Ma et al., 2014; Froscio et al., 1989; Butler et al., 2015; Stallings-Mann et al., 2006). Among those inhibitors, auranofin (ANF) has been widely studied for its application in many type of diseases other than rheumatoid arthritis, including cancer, neurodegenerative diseases, AIDS, parasitic infections and bacterial infections (Roder and Thomson, 2015). In several preclinical studies on cancer treatment, ANF has shown treatment effects on NSCLC, ovarian cancer, GIST and various types of leukemia and lymphoma (Pessetto et al., 2013; Fiskus et al., 2014; Chen et al., 2014).

Previous study has shown that aPKC-ι was overexpressed in CRC and required for oncogenic transformation and carcinogenesis of CRC (Murray et al., 2004). However, the underlying mechanism has not been fully clarified yet. Our study aimed to further investigate the mechanism of aPKC-ι in the tumorigenesis of CRC.

2. Material and methods

2.1. Cell culture and induction of EMT in CRC cell lines

SW480 and HCT116 cell lines were purchased from American Type Culture Collection (Manassas, USA) and cultured in RPMI 1640 (Boster, China) with 10% fetal bovine serum (Sigma Aldrich, USA). Cells were kept at 37 °C in a humidified atmosphere with 5% CO_2 for subsequent analysis. TGF-β1 was purchased from Invitrogen (Thermo Fisher Scientific, USA) and dissolved in PBS with 0.1% bovine serum albumin. TGF-β1 was added to cell culture media at a final concentration of 10 ng/ml, as described in Kong et al. (Kong et al., 2016). MTT cytotoxicity assay.

The cytotoxicity of ANF on SW480 and HCT116 cell lines was evaluated using 3-(4,5)-dimethylthiahiazo (−z-y1)-3,5-di-phenytetrazoliumromide (MTT) assay as described in Ling et al.(Ling et al., 2018). Basically, after reaching the logarithmic growth stage, SW480 and HCT116 cells were treated with ANF (0, 0.1, 0.25, 0.5, 1.0, 2.0, and 5.0 μM), or DMEM (negative control) for 72 h. After the treatment, MTT solution (20 μL, 5 mg/mL) was added and further incubated 4 h at 37 °C. The produced formazan crystals were dissolved by addition of 150 μL DMSO for 10 min. Finally, the absorbance of individual samples was examined at 490 nm.

2.2. Vector construction and transfection

Complete coding sequence of Rac1G12V was obtained from Sangon Biotech (Shanghai, China) and cloned into the pcDNA3.1 vector (Invitrogen, USA). SW480 and HCT116 cell lines were seeded in 6-well culture plates and transfected with 4 μg pcDNA3.1-Rac1G12V or control pcDNA3.1 vector using 10 μl Lipofectamine 2000 (Invitrogen).

Short hairpin RNA (shRNA) targeting aPKC-ι (sh-aPKC-ι) was synthesized by Sangon Biotech (Shanghai, China), with a scramble shRNA (sh-NC) as control. The sequences were as follow, sh-aPKC-ι-1: 5′-CACCGCAATGAGGTTCGAGACATGTTTCAAGAGAACATGTCTCGAACC TCATTGCTTTTTTG-3′, sh-aPKC-ι-2: 5′- CACCGCCACACTTTCCAAGCC AAGCTTCAAGAGAGCTTGGCTTGGAAAGTGTGGCTTTTTG-3′, sh-aPKC-ι-3: 5′- CACCGCACAGACAGTAATTCCATATTTCAAGAGAATATG GAATTACTGTCTGTGCTTTTTTG-3′, sh-NC: 5’-CACCGTTCTCCGAACG TGTCACGTCAAGAGATTACGTGACACGTTCGGAGAATTTTTTG-3′.
SW480 and HCT116 cell lines were transfected with sh-aPKC-ι (3 μg/6-well) or control scramble shRNA (3 μg/6-well) using Lipofectamine 2000 (Invitrogen, USA) according to the manufacturer's instructions. Validation of the gene silencing was performed by quantitative real-time PCR.

2.3. Wound healing assay

Cell migration ability was evaluated using wound healing assay as described in Gunaratne et al.(Gunaratne et al., 2013). Basically, SW480 or HCT116 cells were seeded in 6-well culture plates at 1.5×10^6 cells/well and incubated at 37 °C for 24 h. Cells were then transfected by sh-aPKC-ι or pcDNA3.1-Rac1G12V plasmid for an additional 24-h incubation. The plate was then scratched with a pipette tip to create a “wound”, and the cells were washed three times with PBS, followed by addition of 5% FBS-RPMI 1640 media. For ANF and TGF-β1 treatment, SW480 or HCT116 cells were seeded in 6-well culture plates (Corning, USA) at 1.5×10^6 cells/well. After incubation for 8 h, cells were scratched with a pipette tip. After three washes with PBS to remove the debris, cells were cultured in RPMI 1640 with 0.5 μM ANF for 72 h or with 10 ng/ml TGF-β1 for 48 h, as previously described(Hrabe et al., 2015; Sachweh et al., 2015). Images of the wound were acquired before the scratch and at the indicated time after the scratch using an inverted microscope with digital camera. Width of the wound was calculated using Image J.

2.4. Cell invasion

Cell invasion of SW480 and HCT116 cell lines was further evaluated using transwell assay. The assay was performed using modified Boyden chambers (Transwell, USA). Before the transwell assay, SW480 and HCT116 cell lines were transfected by pcDNA-Rac1, sh-aPKC-ι or sh-NC and then incubated for another 48 h. Sixty micro-liter of 0.23 mg/ml Matrigel (Corning) was used to pre-coat the membranes on the upper chamber. The chamber was then incubated at 37 °C, 5% CO_2, for 2 h to allow the gelling. After equilibrate the chambers with complete media for 1 h, 30,000 cells were seeded into the upper chamber, which were allowed to migrate towards the lower chamber containing RPMI 1640 medium with 10% FBS. After incubation at 37 °C for another 24 h, cells were fixed with 4% paraformaldehyde for 30 min and stained with 1% crystal violet (Sigma). Then the number of cells was counted visually using a microscope in five different fields under ×200 magnifications per filter. Each experiment was performed in triplicate.

For ANF treatment, the transwell assay was performed as described

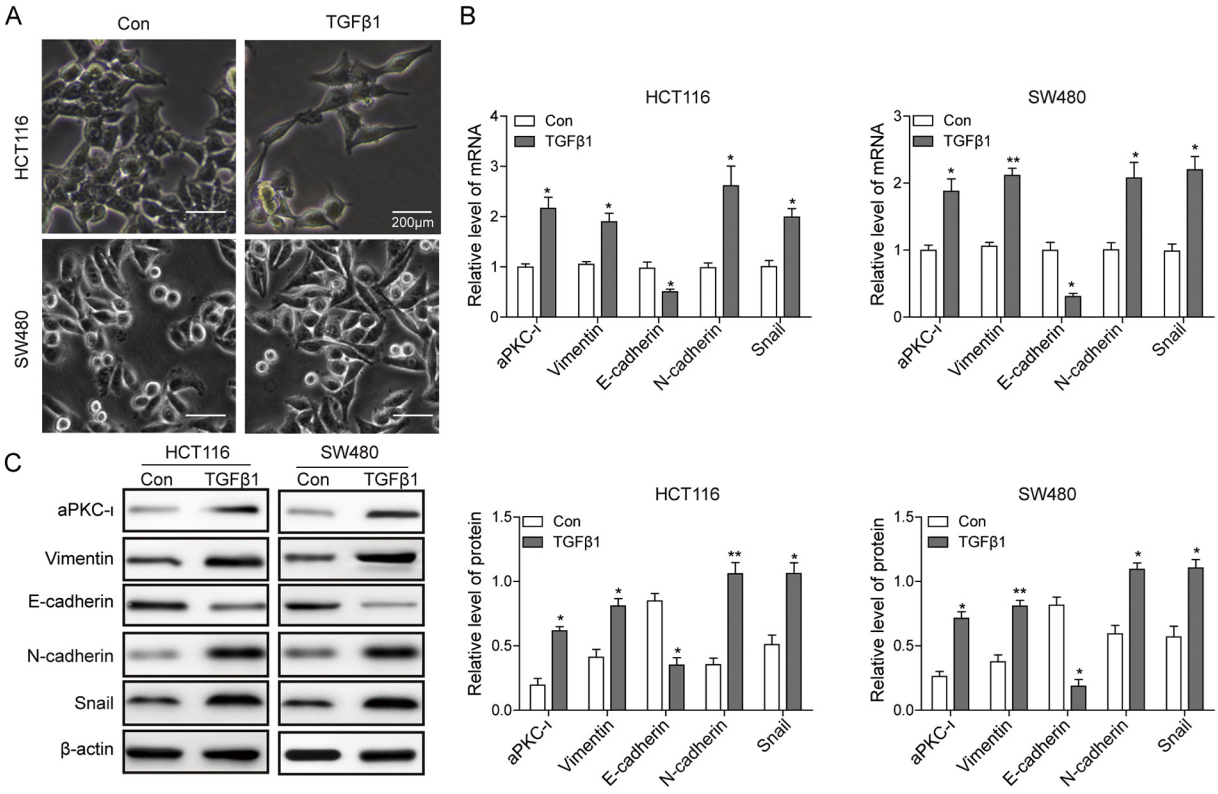

Fig. 1. SW480 and HCT116 cell lines were cultured with RPMI 1640 culture media with or without 10 ng/ml TGF-β1 for 72 h. Morphology of cells was examined under microscope (A). mRNA (B) and protein (C) expression levels of aPKC-ι, E-cadherin, vimentin, Snail and N-cadherinwere measured using quantitative real-time PCR and western blot, respectively. Data were presented as mean ± SD from at least three independent experiments (*$P < .05$, **$P < .01$, compared to control groups).

above, except that the culture medium in the lower chamber were replaced by RPMI 1640 medium with 10% FBS and 0.5 μM ANF.

2.5. Quantitative real-time PCR

Total RNA was extracted from cell samples using TRIzol RNA isolation reagents (Invitrogen, CA, USA) and 1 μg of RNA was reverse-transcribed at 48 °C for 30 min using a Superscript IV reverse transcriptase (Applied Biosystems). Quantitative real-time PCR (q-PCR) was performed using Applied Biosystems 7500 Real-Time PCR System (ABI, USA) as described in Yang et al. (Yang et al., 2016) with the following primers: aPKC-ι sense 5′-TACGGCCAGGAGATACAACC-3′ and anti-sense 5'-CATCTGGAGTGAGCTGGACA-3′; E-cadherin sense 5′-CTGGA CAGGGAGGATTTTGA-3′ and anti-sense 5′-ACCTGAGGCTTTGGATT CCT-3′; vimentin, sense 5′-AGAGAACTTTGCCGTTGAAGC-3′ and anti-sense 5′-ACGAAGGTGACGAGCCATT-3′; N-cadherin sense 5′- AGGGG ACCTTTTCCTCAAGA -3′ and anti-sense 5′-TCAAATGAAACCGGGCT ATC-3′; Snail, sense 5′- GAGCCCAGGCAGCTATTTCA-3′ and anti-sense, 5′- CATCGGTCAGACCAGAGCAC-3′. β-actin sense 5′- GGGAAATCGTG CGTGACATTAAG-3′ and reverse 5′- TGTGTTGGCGTACAGGTCTTTG-3′ was used as the internal reference.

2.6. Western blot

Cytosolic and nuclear extracts of the cancer cells were prepared as described in Wu et al. (Wu et al., 2008). Briefly, trypsinized cells were washed in cold Ca^{2+}- and Mg^{2+}-free PBS and re-suspended in HLB buffer with protease inhibitors for 15 min on ice. The cells were homogenized and centrifuged at 1000 x g, 4 °C for 1 h. The supernatant was stored at −80 °C until use. For the nuclear extracts, the pellet was washed with HLB buffer twice and then extracted with nuclear extraction buffer and stored at −80 °C until use. Cell lysates or nuclear extracts were prepared in 1 x SDS lysis buffer, and boiled for 10 min. Protein contents were then determined using BCA Protein Assay Reagent (Pierce, USA). After being diluted with 1 x lysis buffer, equal amount of protein was loaded onto SDS-polyacrylamide gels (12% acrylamide in separating gel and with 5% in stacking gel) and separated by electrophoresis. Proteins were then transferred to nitrocellulose membranes. After blocking in 5% skimmed milk in PBS at 4 °C overnight, membranes were incubated with anti-aPKC-ι antibody (1:250, #5584, Cell Signaling Technology, USA), anti-E-cadherin antibody (1:500, 20,874–1-AP, ProteinTech Group, USA), anti-vimentin antibody (1:500, 10,366–1-AP, ProteinTech Group, USA), anti-β-actin antibody (1:1000, A5316, Sigma, USA), anti-Rac1 antibody (1:500, ab33186, Abcam, USA), anti-phospho-c-Jun NH2-terminal kinase (JNK) antibody (1:250, #9251, Cell Signaling Technology, USA), anti-JNK antibody (1:500, #4672, Cell Signaling Technology, USA), anti-phosphorylated STAT3 (p-STAT3) antibody (1:250, #98543, Cell Signaling Technology, USA), anti-STAT3 antibody (1:500, ab31370, Abcam, USA), anti-lamin B1 antibody (1:1000, ab16048, Abcam, USA), anti-β-catenin antibody (1:500, ab16051, Abcam, USA) or β-actin antibody(1;3000, ab8226, Abcam, USA) for 2 h. They were then incubated with either goat anti-rabbit IgG (1:2000, ab6721, Abcam, USA) or goat anti-mouse IgG (1:3000, ab97265, Abcam, USA), correspondingly. Protein signals were then visualized using Gel Doc XR + gel documentation system (Bio-Rad, USA).

2.7. Measurement of Rac1 activity

Activity of Rac1 was measured using an EZ-detect Rac1 kit (Pierce Biotechnology) as described in Shen et al.(Shen et al., 2010). Basically, cells were firstly transfected by sh-aPKC-ι or treatment with 0.5 μM for 48 h. The cells were then lysed in lysis buffer (Pierce, USA) containing protease inhibitor cocktail, and the supernatant was collected by

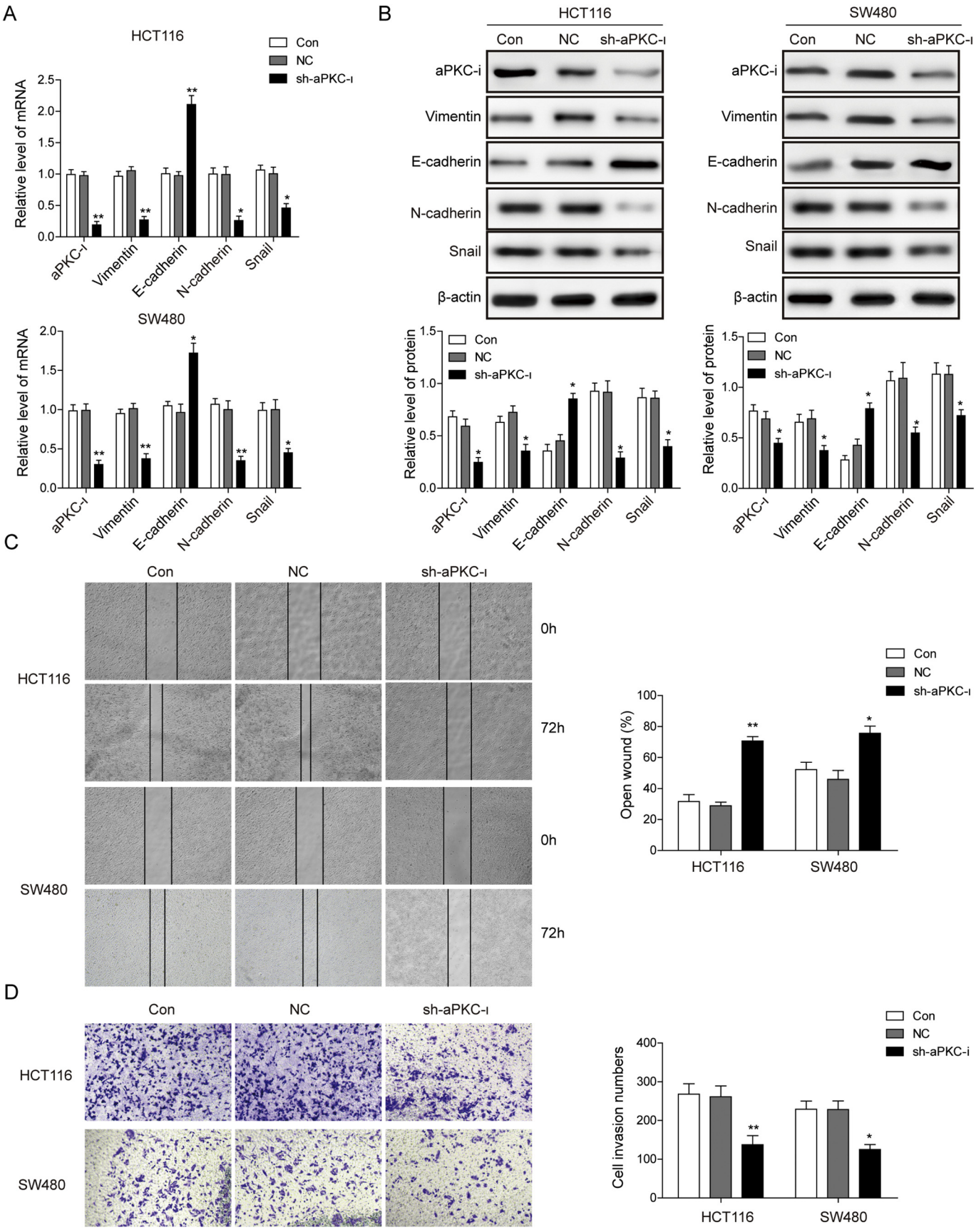

Fig. 2. SW480 and HCT116 cell lines were transfected with sh-aPKC-ı or control scramble shRNA. After transfection for 72 h, expression levels of aPKC-ı, E-cadherin vimentin, Snail and N-cadherin were measured using quantitative real-time PCR (A) and western blot (B). Cell migration (C) and invasion ability (D) were evaluated using wound healing assay and transwell assay, respectively, in both SW480 and HCT116 cell lines. Data were presented as mean ± SD from at least three independent experiments (*$P < .05$, **$P < .01$, compared to sh-NC groups).

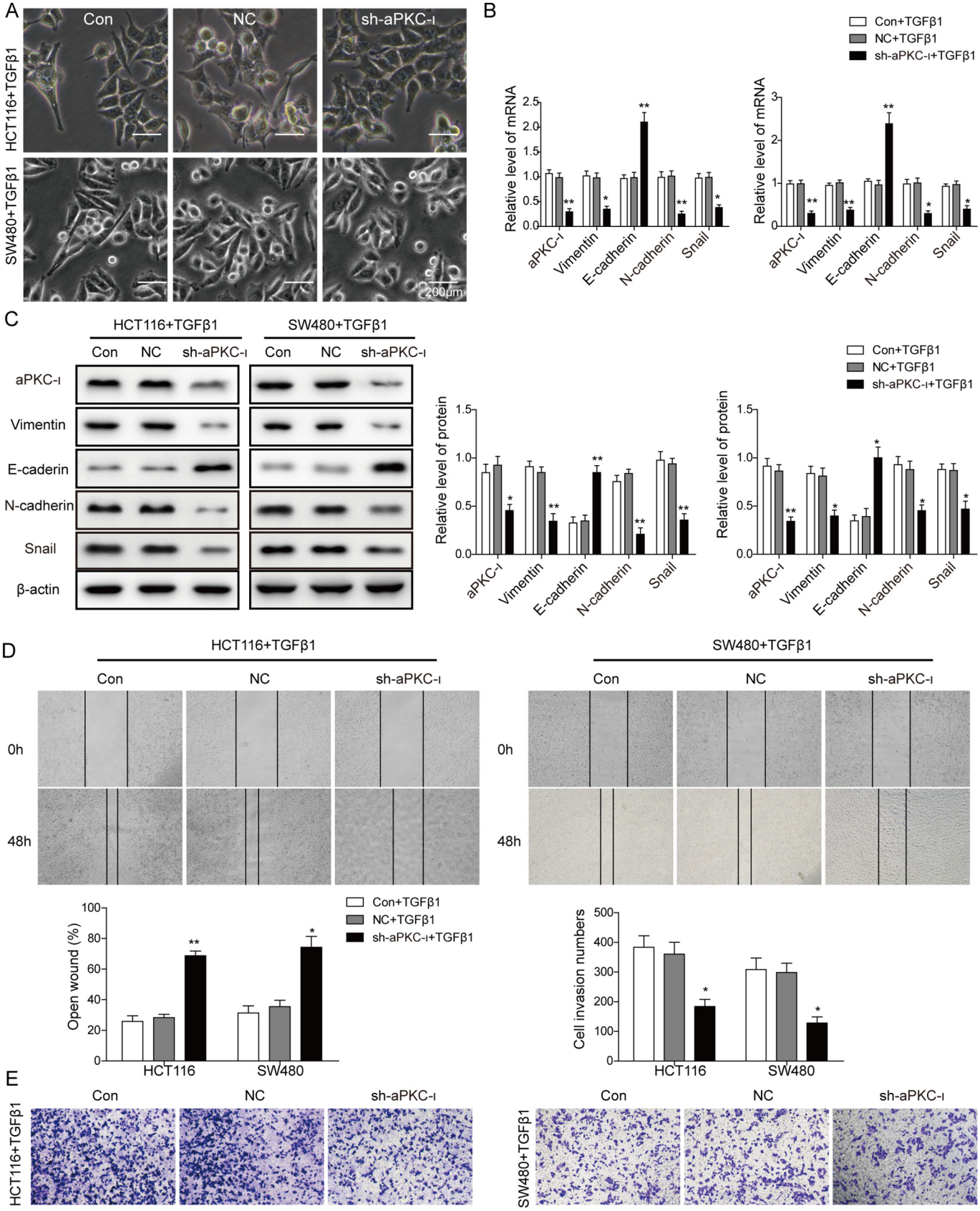

Fig. 3. SW480 and HCT116 cell lines were transfected with 3 μg sh-aPKC-ι or control scramble shRNA, and then treated with 10 ng/ml TGF-β1. Morphology of cells was examined under microscope (A). Quantitative real-time PCR (B) and western blot (C) were used to measure the expression levels of aPKC-ι, E-cadherin and vimentin in both SW480 and HCT116 cell lines, and wound healing assay and transwell assay were used to evaluate cell migration (D) and invasion ability (E), respectively. Data were presented as mean ± SD from at least three independent experiments (*$P < .05$, **$P < .01$, compared to control groups).

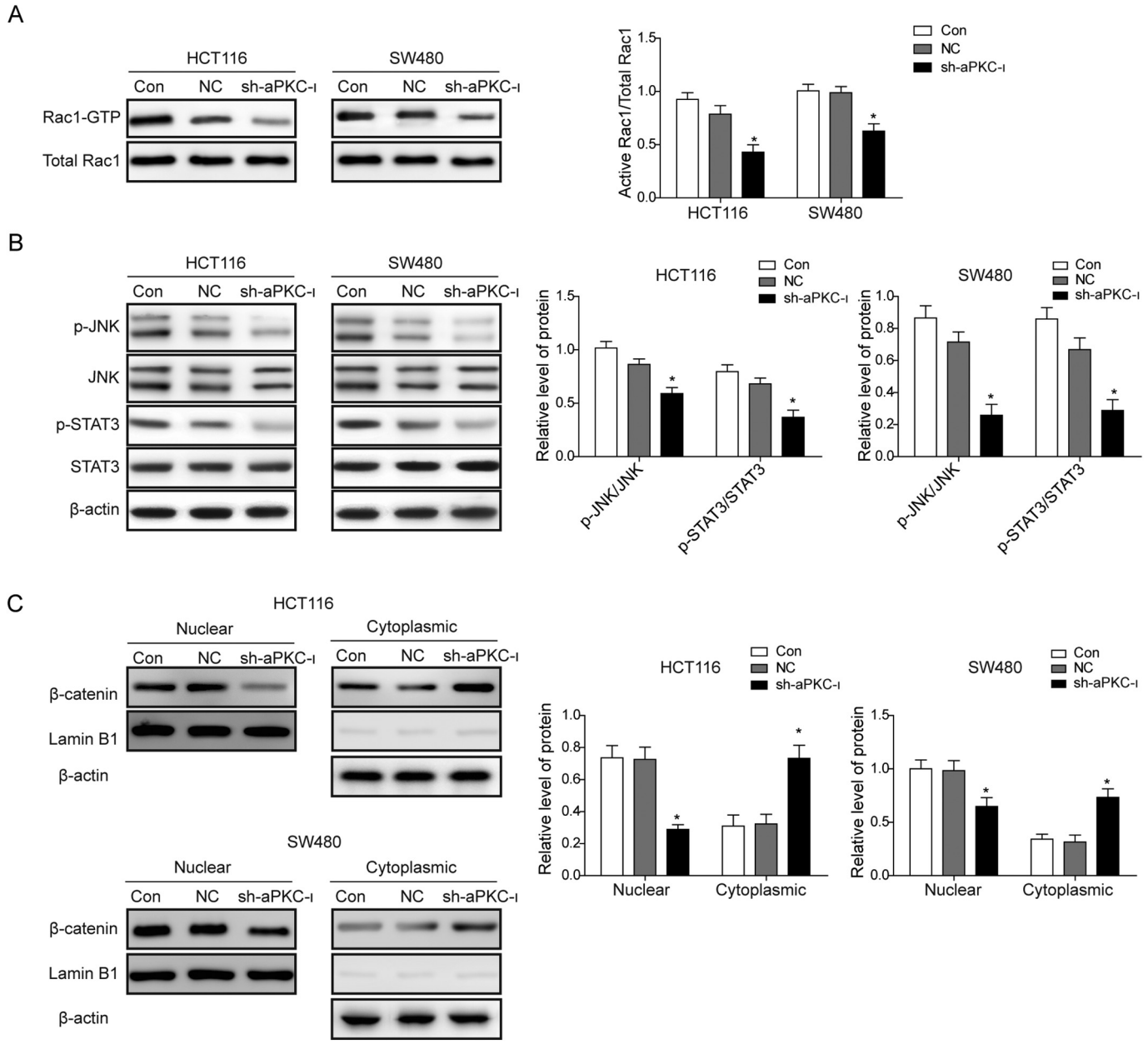

Fig. 4. SW480 and HCT116 cell lines were transfected with sh-aPKC-ι or sh-NC. After 72-h incubation, cells were lysed and activated Rac1 (Rac1-GTP) was precipitated with glutathione S-transferase and detected using western blot (A). Expression of phospho-c-Jun NH2-terminal kinase (p-JNK), phosphorylated STAT3 (p-STAT3) were also measured by western blot. β-actin were used as a loading control (B). Nuclear and cytoplasmic levels of β-catenin were measured using western blot. Lamin B1 and β-actin were used as a loading control of nuclear and cytoplasmic protein, respectively.(C). Data were presented as mean ± SD from at least three independent experiments (*$P < .05$, **$P < .01$, compared to sh-NC).

centrifugation at 16,000 x g, 4 °C for 15 min. Activated Rac1 was then precipitated with glutathione S-transferase and detected by western blot.

2.8. Statistical analysis

Statistical analysis was performed using Graphpad Prism 5. *Student t-test* was used to compare means between two groups, while one-way ANOVA followed by Tukey's comparison analysis was used to compare multiple groups. *$P < .05$, **$P < .01$ was considered statistically significant.

3. Results

3.1. TGF-β1 promoted the expression of aPKC-ι in CRC cells

We firstly investigated the aPKC-ι expression in two CRC cell lines (SW480 and HCT116) after being treated by 10 ng/ml TGF-β1, an EMT inducer in cancer cells(Elliott et al., 2002). As shown in Fig. 1A, both SW480 and HCT116 cell lines have transformed from epithelial phenotype to mesenchymal phenotype, after treatment of TGF-β1 for 72 h. In addition, both mRNA and protein expression of E-cadherin was decreased while the mRNA and protein level of vimentin, Snail and N-cadherin were significantly increased after the TGF-β1 treatment (Fig. 1B & 1C). Moreover, the mRNA and protein expression of aPKC-ι was increased by nearly two folds after the TGF-β1 treatment (Fig. 1B &

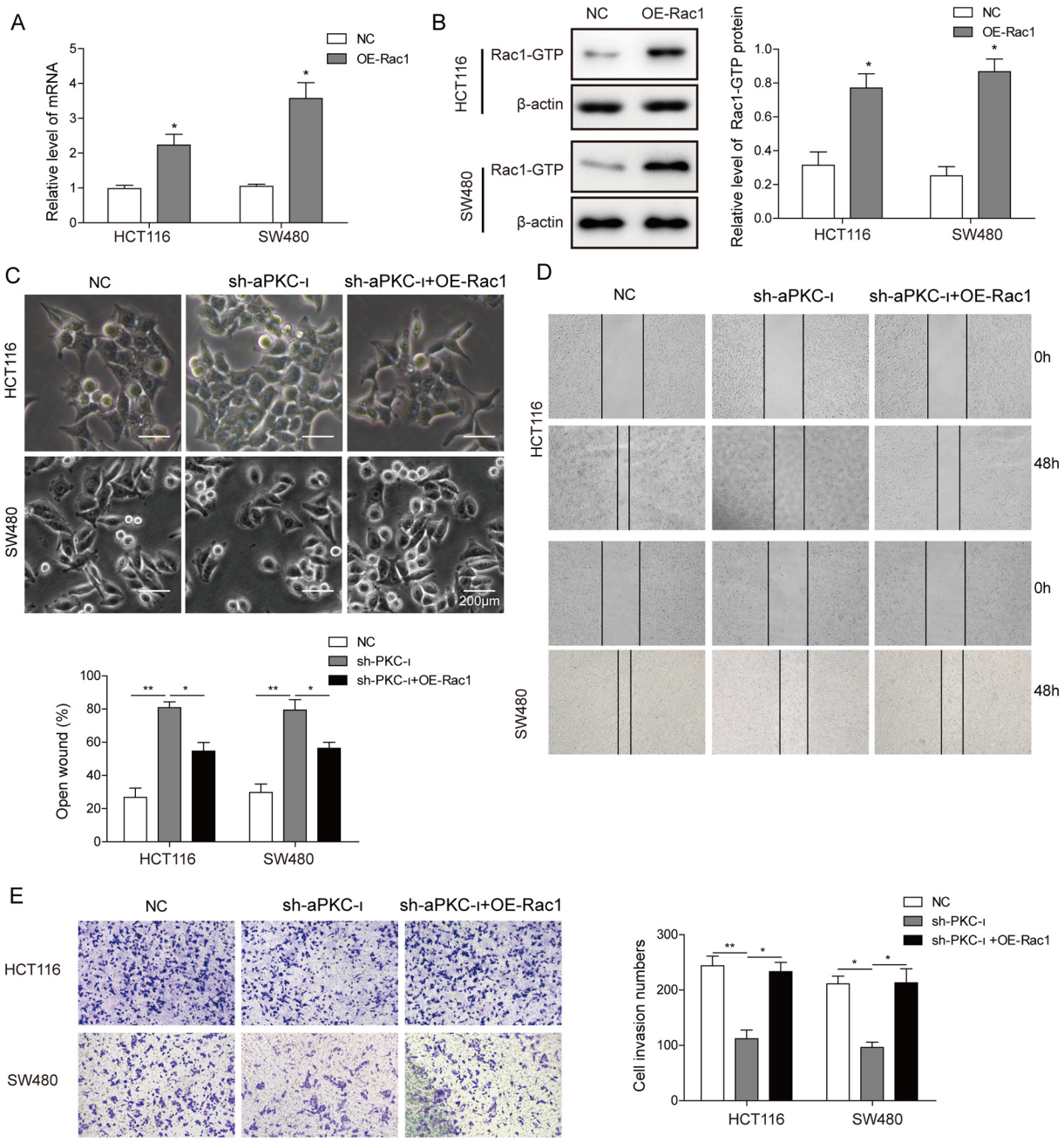

Fig. 5. HCT116 and SW480 cell lines were transfected with pcDNA3.1-Rac1G12V(OE- Rac1) or control pcDNA3.1 vector (NC). After transfection for 48 h, expression levels of Rac-1 were measured using quantitative real-time PCR (A) and western blot (B), and cell morphology of both cell lines was evaluated under microscope, scal bar: 200 μm (C). Cell migration (D) and invasion (E) ability were evaluated using wound healing assay and transwell assay, respectively. Data were presented as mean ± SD from at least three independent experiments (*$P < .05$, **$P < .01$, compared to control groups).

1C), indicating a possible association between aPKC-ι and EMT of CRC cells.

3.2. Knockdown of aPKC-ι inhibited the migration and invasion of CRC cell lines

In order to further investigate the effect of aPKC-ι on the cell migration and invasion, we further knocked down the expression of aPKC-ι using shRNA in both SW480 and HCT116 cell lines. The results showed that the expression levels of aPKC-ι were decreased after shRNA knockdown (Fig. 2A & 2B). In addition, the expression level of E-cadherin was increased, while expression levels of vimentin, Snail and N-cadherin were decreased in both mRNA and protein, compared to control and sh-NC groups (Fig. 2A & 2B). Wound healing assay showed a slower healing after the knockdown of aPKC-ι, compared to control in both cell lines at 72 h (SW480: $P < .05$; HCT116: $P < .01$, Fig. 2C). Transwell assay showed that the number of invaded cells were less in aPKC-ι knockdown group compared to control (SW480: $P < .05$; HCT116: $P < .01$, Fig. 2D). Both wound healing test and transwell assay results indicated an inhibited capability of migration and invasion of those CRC cell lines after the knockdown of aPKC-ι.

3.3. Knockdown of aPKC-ι inhibited TGF-β1-induced EMT, cell migration and invasion

As shown in Fig. 3A, TGF-β1-induced EMT of HCT116 and SW480

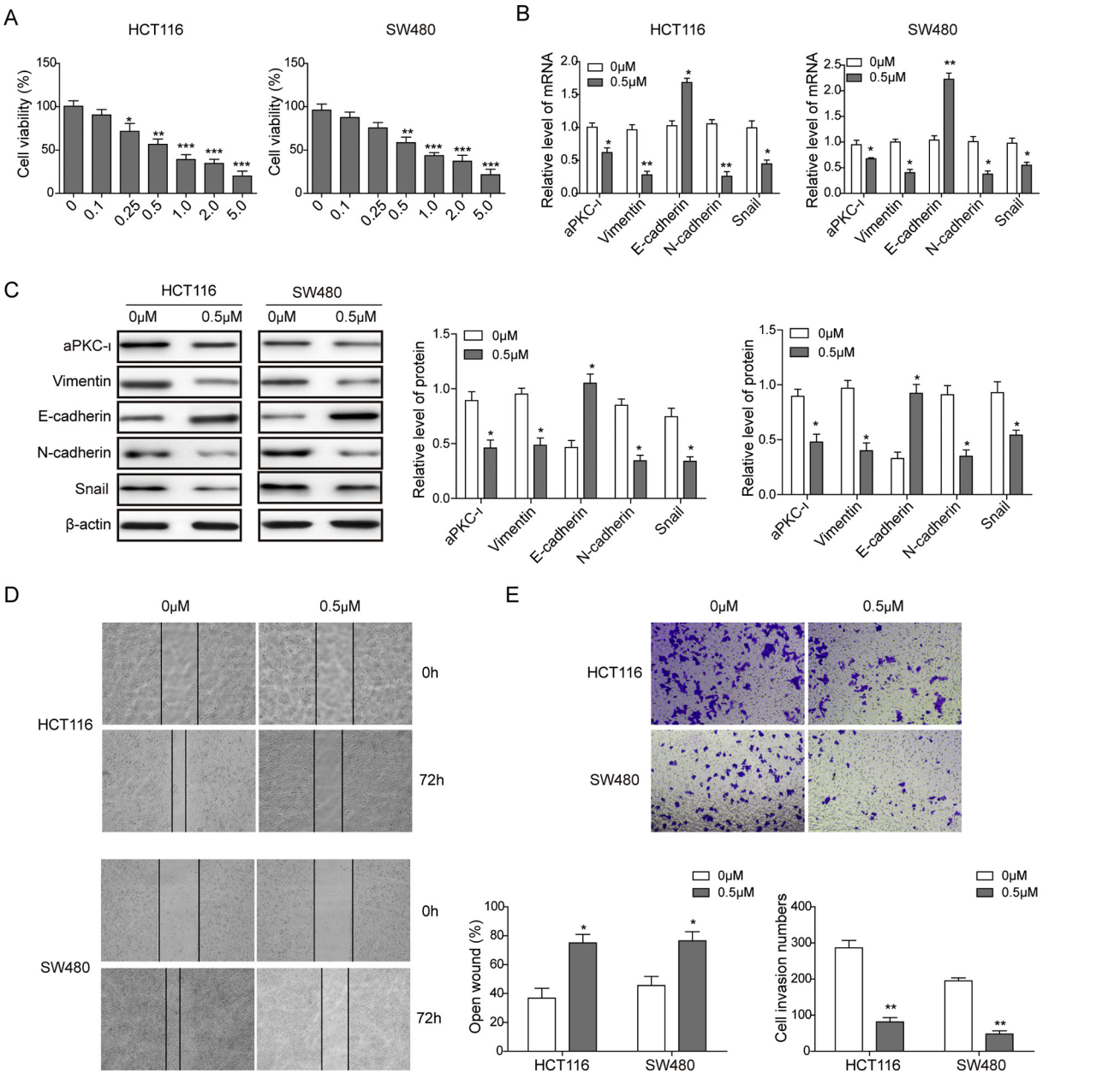

Fig. 6. Influence of ANF on the EMT, invasion and migration of CRC cell lines. (A) MTT assay was used to evaluate the cytotoxicity of ANF in SW480 and HCT116 cell lines. After SW480 and HCT116 cell lines were treated with 0.5 μM auranofin (ANF) for 72 h, mRNA (B) and protein (C) expression levels of aPKC-ι, E-cadherin, and vimentin were measured using quantitative real-time PCR and western blot. Wound healing assay (D) and transwell assay (E) were used to evaluate the migration and invasion ability of both cell lines, respectively. Data were presented as mean ± SD from at least three independent experiments. (*$P < .05$, **$P < .01$).

cell lines was inhibited by knockdown of aPKC-ι. Similarly, knockdown of aPKC-ι also inhibited the promoting effects of TGF-β1 on vimentin, N-cadherin, and Snail expression, as demonstrated in both mRNA and protein levels, accompanied with increased E-cadherin production (Fig. 3B & 3C). Wound healing assay and transwell assay showed that aPKC-ι knockdown inhibited the TGF-β1-induced cell migration and invasion in both HCT116 and SW480 cell lines (Fig. 3D & 3E).

3.4. Knockdown of aPKC-ι decreased the activation levels of Rac1 and the downstream signaling factors, JNK, STAT3, and nuclear accumulation of β-catenin

We then investigated the downstream signaling factors of aPKC-ι. As shown in Fig. 4A, in both SW480 and HCT116, levels of activated Rac1 (Rac-GTP) were decreased in aPKC-ι-knockdown groups (SW480: $P < .05$; HCT116: $P < .05$). In addition, inhibited Rac-1 activation was accompanied with decreased activation of JNK (p-JNK) in both cell lines, which was decreased by nearly 50% compared to control in SW480. Furthermore, the expression of phosphorylated STAT3 significantly down-regulated in both SW480 and HCT 116 with aPKC-ι knockdown (SW480: $P < .05$; HCT116: $P < .05$, Fig. 4B), and the nuclear levels of β-catenin were also decreased in aPKC-ι-knockdown groups, while its cytoplasmic levels were increased (Fig. 4C). Those results suggest that knockdown of aPKC-ι may inhibit the phosphorylation of STAT3 and control the localization of β-catenin through inhibiting Rac1-JNK pathway.

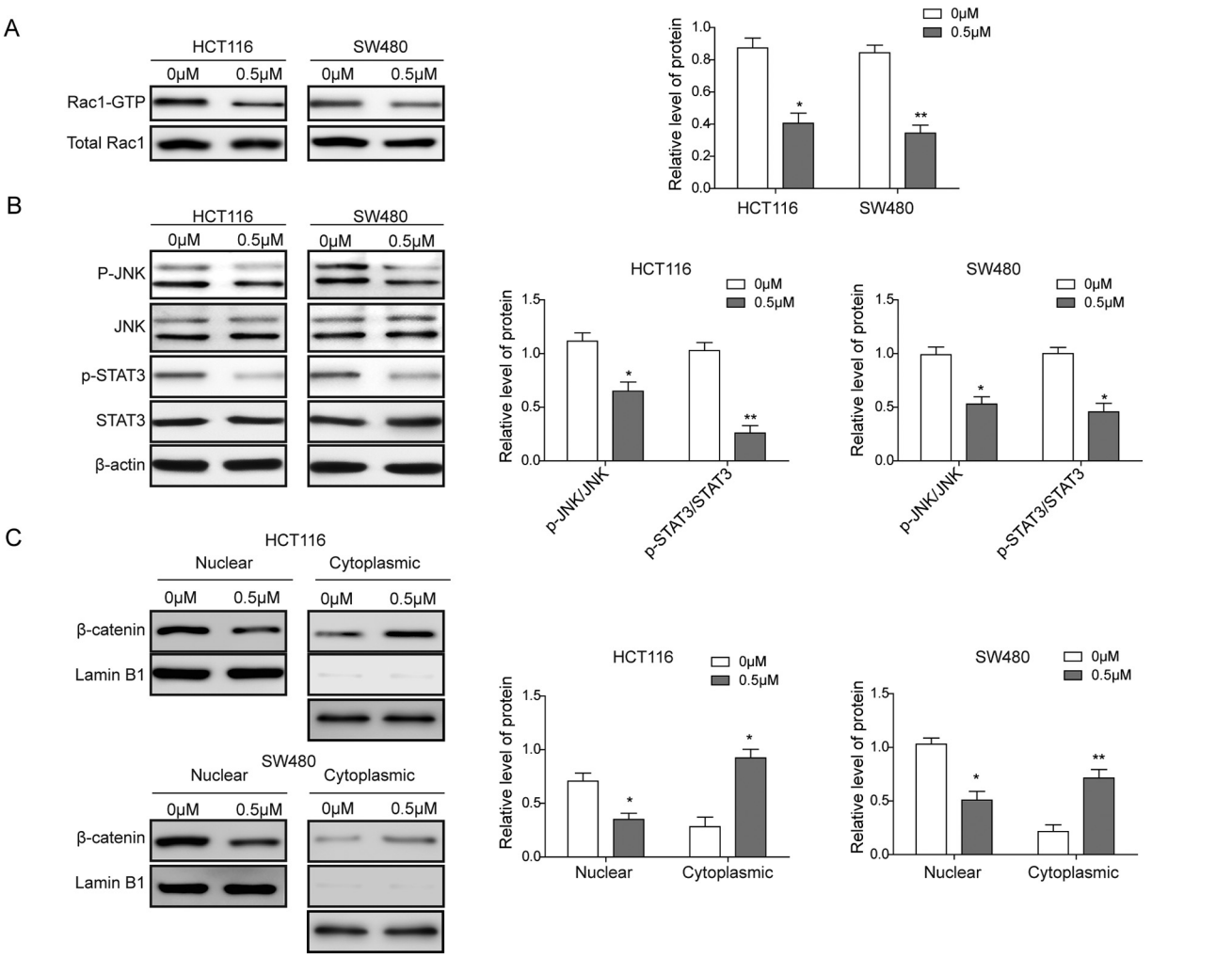

Fig. 7. SW480 and HCT116 cell lines were treated with 0.5 μM auranofin (ANF) for 72 h. After the treatment, levels of activated Rac-1 (Rac-1-GTP) was precipitated with glutathione S-transferase and measured using western blot (A). Levels of phospho-c-Jun NH2-terminal kinase (p-JNK), and phosphorylated STAT3 (p-STAT3) were measured by western blot. β-actin were used as a loading control (B). Nuclear and cytoplasmic levels of β-catenin were measured using western blot. Lamin B1 and β-actin were used as a loading control of nuclear and cytoplasmic protein, respectively(C). Data were presented as mean ± SD from at least three independent experiments (*$P < .05$, **$P < .01$).

3.5. Knockdown of aPKC-ι inhibited the EMT, migration and invasion of CRC cells partially via inhibition of Rac1

To elucidate if the effect of aPKC-ι on CRC cell EMT, migration and invasion is Rac-1 dependent, we transfected the pcDNA-Rac1G12V plasmid into aPKC-ι knockdown cells. As shown in Fig. 5A-5B, expression of *Rac1-GTP* was increased by 2–3 folds in HCT116 and SW480 cell line after overexpressing *Rac1*G12V gene. After the overexpression of Rac1-GTP, both CRC cell lines showed more mesenchymal phenotype and less epithelial phenotype under microscope compared to control, indicating that Rac-1 overexpression partially recovered the inhibited EMT of CRC cell lines by aPKC-ι knocked-down (Fig. 5C). The results of wound healing assay and transwell assay showed a partial recovery of the inhibited effect of aPKC-ι knock-down on cell migration and invasion ability in CRC cells (Fig. 5D & 5E). Overall, those results indicate that aPKC-ι inhibited the migration and invasion of CRC cells partially via the inhibition of Rac1 pathway.

3.6. Influence of ANF on the EMT, invasion and migration of CRC cell lines

In order to further understand the role of aPKC-ι in EMT and metastasis of CRC, we also treated CRC cell lines with an aPKC-ι inhibitor, ANF, and investigated the changes in the EMT, invasion and migration of CRC cell lines. We firstly evaluated the cytotoxicity of ANF on HCT116 and SW480 cell lines, and results showed decreased cell survival with the increase in the concentration of ANF (Fig. 6A), with IC50 near 0.5 μM. Based on the results of ANF cytotoxicity evaluation, we used 0.5 μM ANF in the subsequent experiments. As shown in Fig. 6B and 6C, 0.5 μM ANF slightly decreased the expression levels of aPKC-ι in both CRC cell lines. However, expression of vimentin was significantly deceased, together with an increase in E-cadherin expression levels (Fig. 6C), indicating that EMT of those cell lines could be inhibited by ANF. Wound healing assay and transwell assay showed a slowed healing and decreased number of invasion cells after treatment with ANF, indicating that ANF could inhibit the invasion and migration of CRC cells (Fig. 6D & 6E).

3.7. Influence of ANF on the downstream signaling factors of aPKC-ι

On the presence of 0.5 μM ANF, levels of Rac1-GTP were decreased by nearly 50% in both cell lines (Fig. 7A), together with decreased levels of phosphorylated JNK (SW480: $P < .05$; HCT116: $P < .05$), and the downstream p-STAT3 was also down-regulated compared to control groups (SW480: $P < .05$; HCT116: $P < .01$, Fig. 7B). In addition, nuclear levels of β-catenin were shown to be decreased, while its cytoplasmic levels were increased, on the presence of ANF (Fig. 7C).

Those results indicate that ANF could inhibit the aPKC-ι expression and also the activation of its downstream signaling factor, including Rac1, JNK and STAT3. Nuclear translocation of β-catenin was also restrained by ANF.

4. Discussion

In this study, we have investigated the relationship between aPKC-ι expression level and EMT, migration and invasion of CRC cell lines. After treatment by TGF-β1, an EMT inducer(Elliott et al., 2002), we have observed a successful transition from epithelial phenotype to mesenchymal phenotype in CRC cell lines, both morphologically (from a more polarized epithelial morphology to a more non-polarized mesenchymal morphology, Fig. 1A) and by molecular biomarkers (Fig. 1B & 1C). In those TGF-β1-treated CRC cell lines, expression of aPKC-ι was increased in both mRNA and protein levels (Fig. 1B & 1C), which is consistent with the previous findings that aPKC-ι plays a role in the EMT of cancer(Murray et al., 2011). We further knocked down the expression of aPKC-ι in CRC cell lines, and observed increased expression of E-cadherin and decreased expression of vimentin, Snail, N-cadherin and decreased ability to migrate and invade (Fig. 2). In addition, aPKC-ι knock-down also inhibited the TGF-β1-induced EMT, cell migration and invasion in CRC cell lines (Fig. 3). Those findings further confirmed the role of aPKC-ι in the EMT, migration and invasion of CRC cell lines.

Previous studies have found that aPKC-ι drove the transformed growth of NSCLC by activating Rac-1(Gunaratne et al., 2013; Justilien and Fields, 2009). Similarly, decreased activated Rac-1 (Rac-1-GTP) levels were also observed when aPKC-ι was knocked down in our study (Fig. 4A). In addition, study by Wu et al. found that activated Rac-1 could promote the nuclear translocation of p-STAT3 and β-catenin which was mediated by JNK (Wu et al., 2008). In our study, the downstream pathway factors of Rac1, including JNK, STAT3 and β-catenin, showed decrease in their activated forms, p-JNK, p-STAT3 and nuclear β-catenin, in aPKC-ι-knockdown CRC cell lines (Fig. 4B&4C). In addition, Rac-1 over-expression has partially rescued the inhibition of EMT, cell migration and invasion by aPKC-ι knockdown in CRC cell lines (Fig. 5). Those results indicate that similar to NSCLC, aPKC-ι may also promote the EMT of CRC via Rac1 pathway.

ANF is a member of a group of anti-rheumatoid arthritis drugs which were widely studied for their potential usage in other diseases, including cancer(Roder and Thomson, 2015). Members of this group of drugs have been found to be able to inhibit the EMT of cancer cells through inhibition of aPKC-ι, e.g. aurothiomalate (ATM) in pancreatic cancer(Butler et al., 2015) and HCC(Ma et al., 2014), aurothioglucose (ATG) in NSCLC(Stallings-Mann et al., 2006), and ANF was also shown to inhibit PKC-ι signaling in ovarian cancer(Wang et al., 2013). Since ATM and ATG are no longer available for clinical usage, we instead evaluated the effect of ANF and its possible role in CRC treatment. Although only slightly decreasing the expression level of aPKC-ι, ANF showed similar inhibition on the EMT, migration and invasion of CRC cell lines (Fig. 6) as aPKC-ι knockdown (Fig. 2). These data could be partially explained by the previous findings by Wang et al. that ANF could inhibit aPKC-ι by influencing the interaction between aPKC-ι and Par6, while no inhibition on aPKC-ι expression were observed in ovarian cancer cells(Wang et al., 2013). In addition, the results showed that similar to the results of aPKC-ι knockdown, ANF also inhibited the activation of downstream signaling factors of the aPKC-ι-Rac1-JNK pathway (Fig. 7). All those results indicate that ANF could inhibit the EMT, migration and invasion of CRC cell lines via inhibition of aPKC-ι and the downstream Rac1-JNK pathway.

5. Conclusions

In conclusion, this study demonstrated that aPKC-ι plays important roles in the EMT, migration and invasion of CRC cell lines. By activating Rac-1, aPKC-ι could facilitate the phosphorylation of the downstream signaling factor, JNK, which then promotes the phosphorylation of STAT3 and nuclear translocation of β-catenin, eventually leading to the EMT, migration and invasion of CRC cells. As an inhibitor of aPKC-ι, ANF could inhibit the EMT, migration and invasion of CRC cells by inhibiting the activation of aPKC-ι-Rac1-JNK pathway, which could serve as a potential drug for early prevention of CRC metastasis. Future studies would be required to further investigate the role of aPKC-ι in in vivo metastasis of CRC, as well as the possible role of aPKC-ι knock-down in CRC treatment.

Funding

This work was supported by the National Natural Science Foundation (No: 81770524, No.81470803).

Conflict of interest

The authors declare that they have no conflict of interest.

References

Bosco, R., et al., 2011. Fine tuning of protein kinase C (PKC) isoforms in cancer: shortening the distance from the laboratory to the bedside. Mini Rev Med Chem 11 (3), 185–199.
Butler, A.M., et al., 2015. A small molecule inhibitor of atypical protein kinase C signaling inhibits pancreatic cancer cell transformed growth and invasion. Oncotarget 6 (17), 15297–15310.
Chen, X., et al., 2014. Anti-rheumatic agent auranofin induced apoptosis in chronic myeloid leukemia cells resistant to imatinib through both Bcr/Abl-dependent and -independent mechanisms. Oncotarget 5 (19), 9118–9132.
Chiappa, A., et al., 2009. The management of colorectal liver metastases: Expanding the role of hepatic resection in the age of multimodal therapy. Crit Rev Oncol Hematol 72 (1), 65–75.
Cho, Y.B., et al., 2012. CC chemokine ligand 7 expression in liver metastasis of colorectal cancer. Oncol. Rep. 28 (2), 689–694.
De Greef, K., et al., 2016. Multisciplinary management of patients with liver metastasis from colorectal cancer. World J. Gastroenterol. 22 (32), 7215–7225.
Du, G.S., et al., 2009. Expression of P-aPKC-iota, E-cadherin, and beta-catenin related to invasion and metastasis in hepatocellular carcinoma. Ann. Surg. Oncol. 16 (6), 1578–1586.
Elliott, B.E., et al., 2002. The role of hepatocyte growth factor (scatter factor) in epithelial-mesenchymal transition and breast cancer. Can. J. Physiol. Pharmacol. 80 (2), 91–102.
Fiskus, W., et al., 2014. Auranofin induces lethal oxidative and endoplasmic reticulum stress and exerts potent preclinical activity against chronic lymphocytic leukemia. Cancer Res. 74 (9), 2520–2532.
Froscio, M., Murray, A.W., Hurst, N.P., 1989. Inhibition of protein kinase C activity by the antirheumatic drug auranofin. Biochem. Pharmacol. 38 (13), 2087–2089.
Garden, O.J., et al., 2006. Guidelines for resection of colorectal cancer liver metastases. Gut 55 (Suppl. 3), iii1–8.
Gunaratne, A., Thai, B.L., Di Guglielmo, G.M., 2013. Atypical protein kinase C phosphorylates Par6 and facilitates transforming growth factor beta-induced epithelial-to-mesenchymal transition. Mol. Cell. Biol. 33 (5), 874–886.
Gurzu, S., et al., 2016. Systematic review of the old and new concepts in the epithelial-mesenchymal transition of colorectal cancer. World J. Gastroenterol. 22 (30), 6764–6775.
Hrabe, J.E., et al., 2015. Disruption of thioredoxin metabolism enhances the toxicity of transforming growth factor beta-activated kinase 1 (TAK1) inhibition in KRAS-mutated colon cancer cells. Redox Biol. 5, 319–327.
Isakov, N., 2018. Protein kinase C (PKC) isoforms in cancer, tumor promotion and tumor suppression. Semin. Cancer Biol. 48, 36–52.
Jain, K., Basu, A., 2014. Protein Kinase C-epsilon Promotes EMT in Breast Cancer. Breast Cancer (Auckl.) 8, 61–67.
Justilien, V., Fields, A.P., 2009. Ect2 links the PKCiota-Par6alpha complex to Rac1 activation and cellular transformation. Oncogene 28 (41), 3597–3607.
Kong, J., et al., 2016. Long non-coding RNA LINC01133 inhibits epithelial-mesenchymal transition and metastasis in colorectal cancer by interacting with SRSF6. Cancer Lett. 380 (2), 476–484.
Kovecsi, A., et al., 2017a. PKCtheta utility in diagnosing c-KIT/DOG-1 double negative gastrointestinal stromal tumors. Oncotarget 8 (34), 55950–55957.
Kovecsi, A., et al., 2017b. Paradoxical expression pattern of the epithelial mesenchymal transition-related biomarkers CD44, SLUG, N-cadherin and VSIG1/Glycoprotein A34 in gastrointestinal stromal tumors. World J Gastrointest Oncol 9 (11), 436–443.
Ling, L., et al., 2018. High Loading, Reversible Disulfide Core-Cross-Linked Multifunctional Micelles for Triggered Release of Camptothecin. Mol. Pharm. 15 (12), 5479–5492.
Ma, C.Q., et al., 2014. The aPKCiota blocking agent ATM negatively regulates EMT and invasion of hepatocellular carcinoma. Cell Death Dis. 5, e1129.

Mjaatvedt, C.H., Markwald, R.R., 1989. Induction of an epithelial-mesenchymal transition by an in vivo adheron-like complex. Dev. Biol. 136 (1), 118–128.
Murray, N.R., et al., 2004. Protein kinase Ciota is required for Ras transformation and colon carcinogenesis in vivo. J. Cell Biol. 164 (6), 797–802.
Murray, N.R., Kalari, K.R., Fields, A.P., 2011. Protein kinase Ciota expression and oncogenic signaling mechanisms in cancer. J. Cell. Physiol. 226 (4), 879–887.
Pessetto, Z.Y., et al., 2013. Drug repurposing for gastrointestinal stromal tumor. Mol. Cancer Ther. 12 (7), 1299–1309.
Roder, C., Thomson, M.J., 2015. Auranofin: repurposing an old drug for a golden new age. Drugs R D 15 (1), 13–20.
Sachweh, M.C., et al., 2015. Redox effects and cytotoxic profiles of MJ25 and auranofin towards malignant melanoma cells. Oncotarget 6 (18), 16488–16506.
Shen, Y., et al., 2010. Toll-like receptor 2- and MyD88-dependent phosphatidylinositol 3-kinase and Rac1 activation facilitates the phagocytosis of Listeria monocytogenes by murine macrophages. Infect. Immun. 78 (6), 2857–2867.
Stallings-Mann, M., et al., 2006. A novel small-molecule inhibitor of protein kinase Ciota blocks transformed growth of non-small-cell lung cancer cells. Cancer Res. 66 (3), 1767–1774.
Thiery, J.P., 2003. Epithelial-mesenchymal transitions in development and pathologies. Curr. Opin. Cell Biol. 15 (6), 740–746.
Villalba, M., et al., 2017. Role of TGF-beta in metastatic colon cancer: it is finally time for targeted therapy. Cell Tissue Res. 370 (1), 29–39.
Wang, Y., Hill, K.S., Fields, A.P., 2013. PKCiota maintains a tumor-initiating cell phenotype that is required for ovarian tumorigenesis. Mol. Cancer Res. 11 (12), 1624–1635.
Wu, X., et al., 2008. Rac1 activation controls nuclear localization of beta-catenin during canonical Wnt signaling. Cell 133 (2), 340–353.
Yang, Y., et al., 2016. 14–3-3zeta and aPKC-iota synergistically facilitate epithelial-mesenchymal transition of cholangiocarcinoma via GSK-3beta/Snail signaling pathway. Oncotarget 7 (34), 55191–55210.
Zhu, Q.C., et al., 2013. Epithelial-mesenchymal transition and its role in the pathogenesis of colorectal cancer. Asian Pac. J. Cancer Prev. 14 (5), 2689–2698.